Journal of Environmental Chemical Engineering 9 (2021) 106436

Contents lists available at ScienceDirect

Journal of Environmental Chemical Engineering

journal homepage: www.elsevier.com/locate/jece

Co-pyrolysis of biomass and plastic wastes: A review on reactants synergy, catalyst impact, process parameter, hydrocarbon fuel potential, COVID-19

Khursheed B. Ansari [a,*], Saeikh Zaffar Hassan [b], Rohidas Bhoi [c,d], Ejaz Ahmad [e]

[a] Department of Chemical Engineering, Zakir Husain College of Engineering and Technology, Aligarh Muslim University, Aligarh 202002, India
[b] Department of Petroleum Studies, Zakir Husain College of Engineering and Technology, Aligarh Muslim University, Aligarh 202002, India
[c] Department of Chemical Engineering, Malaviya National Institute of Technology Jaipur, Rajasthan, India
[d] Department of Chemical Engineering, Indian Institute of Technology Bombay, Powai, Mumbai 400076, Maharashtra, India
[e] Department of Chemical Engineering, Indian Institute of Technology (Indian School of Mines), Dhanbad 826004, Jharkhand, India

ARTICLE INFO

Editor: Teik Thye Lim

Keywords:
Biomass and plastic/COVID-19 waste
Co-pyrolysis
Synergistics effect
Catalyst
Reactor parameter
Economic analysis

ABSTRACT

Unprecedented growth in mixed plastic and biomass wastes such as plastic bags, drinking water bottles, agro-and-forestry-waste, along with COVID-19 driven waste (facemask, gloves, PPE kits, surgical masks) have obliged the scientific community to look for technologies that can process and convert both biomass and plastic wastes together into useful end-products. The co-pyrolysis of biomass and plastic would be promising as it may produce a high-quality liquid fuel (hydrocarbon-rich bio-oil) because of the synergy between the two reactants. Notably, the addition of catalysts in a co-pyrolysis process facilitates multiple parallel reactions such as depolymerization, dehydration, deoxygenation, hydrogenation, hydrodeoxygenation, aromatization, and condensation. As a result, hydrocarbon-rich bio-oil, suitable for direct use/blend in the existing fuel, is produced. This review critically discussed the progress and opportunities of co-pyrolysis for the processing of biomass and plastics wastes. Synergistic effects of biomass and plastic during co-pyrolysis, with and without catalyst, are discussed and correlated with the final product yields. Several commercial, naturally occurring metal salts, and anthropogenic catalysts affecting bio-oil yield and composition are reviewed. The mechanistic insight into biomass/plastic thermal decomposition is presented and compared with those under the catalytic environment. Finally, the process parameters and techno-economic analysis of the biomass and plastic co-pyrolysis, including COVID-19 waste handling, are discussed. Co-pyrolysis advised as a promising route for biomass and COVID-19 waste processing and hence management.

1. Introduction

The vast generation of biomass and plastic wastes is creating a great challenge to humankind. The forestry and agricultural residues, horticultural trash, sludge, paper, and pulp are the potential biomass wastes. On the other hand, domestic and food packaging, household appliances, automobile, construction, agriculture, and chemical industries generate a significant quantity of plastic wastes, which has increased enormously in recent years. From over 350 billion tons/year of plastic production across the globe, about 100 billion tons of plastic/year remains untreated and hence disposed of as a landfill. In India, about 15 million tons of plastic waste is generated every year, from which only 3.75 million tons of plastic is recycled due to a poor solid waste management system. Several technologies capable of converting biomass and plastic wastes into useful end-products in a shorter period include gasification and pyrolysis (with and without catalyst) [1–4]. However, implementing such technologies requires the segregation of plastic wastes from other household waste, making large-scale implantation a challenging task. Especially in developing and underdeveloped countries, where most of the population lives in rural areas, it would be challenging to implement such technologies for two reasons. The first reason is associated with the amount of waste generated and the need to install a waste processing unit. Since most localities consist of a very small population, the waste generated is expected to be lower than required to operate an independent unit, thereby requiring the transportation of such waste to a centralized unit mostly located far away from the village. The second most evident problem is the social behavior and lack of awareness among the rural population that usually dump all kinds of biomass and plastic wastes to landfill sites or burn to eliminate it. In case

* Corresponding author.
E-mail address: akabadruddin@myamu.ac.in (K.B. Ansari).

https://doi.org/10.1016/j.jece.2021.106436
Received 2 July 2021; Received in revised form 4 September 2021; Accepted 20 September 2021
Available online 23 September 2021

Nomenclature

COVID-19	Coronavirus disease 2019
PPE	Personal protective equipment
TGA	Thermogravimetric analysis
Ca	Calcium
Mg	Magnesium
Na	Sodium
K	Potassium
ZSM-5	Zeolite Socony Mobil-5
HZSM-5	Protonic type-Zeolite Socony Mobil-5
5-HMF	5-Hydroxymethylfurfural
CO	Carbon monoxide
CO_2	Carbon dioxide
Al-MCM-41	Mesoporous silicates
CeO_2	Cerium oxide
ZnO	Zinc oxide
CaO	Calcium oxide
Fe_2O_3	Iron oxide
MgO	Magnesium oxide
Py-GC/MS	Pyrolysis–gas chromatography–mass spectrometry
USY	Ultrastable Y zeolite
CoNiB	Cobalt nickel boron
NiB	Nickel boron
CoB	Cobalt boron
PVP-CoNiB	Polyvinylpyrrolidone-stabilized CoNiB
P/Ni/ZSM-5	P/Ni supported ZSM-5
PVC	Polyvinyl chloride
LLDPE	Linear low-density polyethylene
DTG	Derivative thermogravimetry
Co/ZSM-5	Cobalt-ZSM-5

the waste is dumped at the designated dumping site, a mobile waste handling unit could be one possibility [5]. Noteworthy that the burning of solid biomass waste remains a common practice and a significant reason for several environmental problems. Further, the plastic waste and the possible direct burning and incineration of biomass waste arising from the agricultural sector may become a severe environmental concern in most developing and underdeveloped nations. Additional discussion on existing biomass and plastic waste issues is provided elsewhere [6–8].

Interestingly, because of its chemical composition, the lignocellulosic biomass is considered an attractive replacement for fossil fuels and can create a closed carbon loop, thereby minimizing greenhouse gases in the atmosphere [9]. Moreover, it can serve as an excellent feedstock to produce value-added chemicals (viz. alcohols, aldehydes, ketones, acids, furans, anhydrosugars, phenols, etc.) besides fuel production [3,10]. In this regard, pyrolysis of waste biomass has shown maximum potential for liquid fuel production (as bio-oil) because of ease of operation and less complexity in the system. The facile pyrolysis technique can also convert waste biomasses such as sludge into hydrocarbon-rich bio-oil [11,12]. In contrast, the pyrolysis-derived bio-oil cannot be utilized directly in the existing engines. One possible reason is the high oxygen content, corrosive nature, and instability of bio-oil, resulting from cellulose/hemicellulose conversion via depolymerization, dehydration, retro-aldol reactions, cyclic-Grob fragmentation, isomerization, etc. reactions [13]. The other explanation can be ascribed to the presence of numerous aromatics components arising from lignin's depolymerization. Therefore, the produced bio-oil from pyrolysis necessarily requires upgradation using a hydrogen source and a catalyst, which makes the process very complicated and expensive, or it is used in small quantities for blending purposes. This could probably be one reason for the limited acceptance of the biomass pyrolysis process, albeit several commercial units exist around the world, mainly in a centralized manner.

In contrast to biomass waste, the fuel produced from the polymeric waste is generally high in H/C content and almost negligible oxygen content, making it a perfect fit for engines. The hydrogen to carbon ratio (H/C) plays a vital role in transforming biomass into hydrocarbons, and plastic is primarily used to increase the H/C ratio. For example, the hydrogen to carbon ratio (H/C) of lignin is 0–0.3. Biomass is deficient in hydrogen; hence co-pyrolysis with plastic (as a hydrogen donor) maximizes the yields of aromatic hydrocarbons. Notably, co-pyrolysis can be used to enhance the H/C ratio and minimize the O/C ratio of the fuel produced from the lignocellulosic biomass. It is be noted that co-pyrolysis is not just mixing to the feedstocks; it changes the whole kinetics, reaction mechanism, operating condition, and hence, the yields of the final pyrolysis product, which forms the basis of this review. Although some reports have discussed co-pyrolysis of biomass and plastic, they are mainly concentrated on either reaction mechanism or process [14–16]. However, a comprehensive review including mechanistic insights on feed decomposition and product formation during biomass and plastic co-pyrolysis, synergistic effect of biomass and plastic-derived compounds during co-pyrolysis, the impact of catalyst on the synergistic, process parameters, and economic aspects of biomass/plastic/COVID-19 wastes is rarely presented.

Further, the positive effects of biomass and plastic co-pyrolysis (forming hydrocarbon-rich products), gives the motivation for COVID-19 waste co-pyrolysis with biomass (or vice versa) to valuable hydrocarbons and chemicals [17]. It is a known fact that the COVID-19 pandemic situation has instigated a devastating effect on human beings' lifestyles. The second wave of COVID-19 has struck the world badly, claiming millions of lives. With over 218 million confirmed cases and more than 4.5 million deaths reported globally, the management and treatment of COVID-19 have caused a drastic surge in the generation of solid waste such as face masks, PPE kits, sanitizer bottles, hand gloves, and other personal hygiene-related items in addition to existing biomass and plastic wastes [18]. The disposal and treatment of COVID-19 waste created new challenges for humankind and the research fraternity. Therefore, this review revisits different technologies based on co-pyrolysis biomass and plastics and elucidates the catalytic and mechanistic insights of such processes. It also explores the potential of COVID-19 waste management through co-pyrolysis because of the similar nature of reactant (or COVID-19 waste) to that of biomass and plastics. Although the volume of waste biomass production per year remains very high compared to COVID-19 waste, there exists an opportunity to co-pyrolyze the waste material in a decentralized manner. Moreover, a great attention has been given to the co-pyrolysis processes that resemble plastic feed composition with solid waste from the non-infected COVID-19 population. We understand that this critical review will provide an insight into the co-pyrolysis process, not only to the researchers working in this area but also to policymakers and social scientists working on COVID-19, energy and environment, rural population, academicians, and scientists.

2. Thermogravimetric analysis (TGA) and co-pyrolysis reactors

The pyrolysis process mainly contains four critical aspects that control the distribution of products (i.e., biochar, bio-oil, and non-condensable gas): (i) reactor technology, (ii) feedstock type/composition, (iii) catalytic/non-catalytic process, and (iv) process parameters like operating temperature, pressure, heating rate, volatiles residence time, particle size, etc. [19]. A comprehensive review of the historical development of pyrolysis reactors for biomass has been published in the literature [20]. Further, a thorough review was reported on the effect of

various reactor configurations on the product distribution in biomass pyrolysis [19,21]. Ahmed et al. [22] and Zhang et al. [23] on co-pyrolysis of biomass and polymer or hydrogen-rich feedstocks suggested that the type of reactors remained specific to the biomass co-pyrolysis process. As per present knowledge, there is no such detailed review available on the effect of reactor configurations on co-pyrolysis of lignocellulosic biomass and plastics. Reactor technology, i.e., the reactor's configuration, governed the heat and mass transfer processes during biomass and plastic co-pyrolysis. Rapid heat transfer to and among the feedstock particles from the heat source and controlled interaction among the solid, liquid, and gas phases during pyrolysis process remained highly desirable. High yield of liquid products (or bio-oil) could be produced by (i) suppressing the secondary char formation via secondary reactions between high molecular weight volatiles, primary products of co-pyrolysis, and pyrolyzing solid matrix [24] and (ii) operating reactor at moderate temperature to avoid further thermal cracking of volatiles into non-condensable gaseous molecules. Therefore, in this section, results of thermogravimetric analysis (TGA) are used to describe the characteristics of thermal degradation of biomass and plastics co-pyrolysis and effects of process parameters such as the blend ratio, operating temperature, and heating rate on the co-pyrolysis. The information from the TGA of blends is then used to correlate the reactivity (R_M), synergistic effects, process parameters, and yield and quality of bio-oil and, finally, the correlation obtained is validated in the different co-pyrolysis reactors. It is suggested that yield and quality of bio-oil in co-pyrolysis reactor can directly correspond to the R_M value determined from TGA.

2.1. Thermogravimetric analysis (TGA) and process parameters

TGA data for independent plastic and biomass pyrolysis and their blend co-pyrolysis are provided in Tables S1–S3, respectively (Supporting information). From the TGA information of plastic pyrolysis in Table S1, the general range of decomposition temperatures of common plastics are arranged and tabulated in Table 1. In PE, PP, PS, and PET, the thermal decomposition range covered from 330 to 550 °C with one peak, whereas in PVC, it remained from 230 to 580 °C with two peaks [25]. Further, the comparison of DTG peak temperature of common plastics at the heating rate of 10 °C min^{-1} given in Table S1 suggested that the ease of decomposition followed PS ≥ PET > PP > LDPE ≥ LLDPE > HDPE > PC order. A similar trend, even at a significantly higher heating rate of 1000 °C min^{-1}, reported in another study, as shown in Fig. S1. TGA study revealed that the biomass pyrolysis proceeded in three major stages viz. drying (up to 150 °C), devolatilization (or active pyrolytic stage over 150–400 °C where cellulose and hemicelluloses decomposed to produced maximum volatiles), and char formation (or passive pyrolytic > 400 °C). Order of decomposition temperature remained as: hemicellulose < cellulose < lignin. Table S3 presents ranges of degradation temperature for second and third stages for various biomasses at different heating rates.

2.1.1. Catalytic and non-catalytic co-pyrolysis of blends

From Table S3, it is evident that the 150–400 °C range was dominated by cellulose and hemicellulose decomposition and 330–550 °C range was dominated by plastic decomposition; these ranges are mentioned as Phase-I and Phase-II, respectively, henceforth. Fig. 1(a) showed the DTG curve for the co-pyrolysis of Doughlas fir sawdust and LDPE [26]. DTG curve showed one peak when Doughlas-fir or LDPE alone pyrolyzed, within their decomposition range, whereas two peaks were observed for Doughlas-fir and LDPE blend. A similar pattern was observed for co-pyrolysis of pinewood sawdust with HDPE and PP [27], wheat straw with PS [28], and Samanea saman seeds with PET [29]. However, the DTG curve of blend would slightly shifted to a lower or

Table 1
General range of decomposition temperature of common plastics.

Plastics	Decomposition temperature range (°C)	No. of peak
LLDPE	280–520	1 peak
LDPE	340–520	1 peak
HDPE	370–550	1 peak
PP	350–520	1 peak
PS	350–550	1 peak
PET	350–520	1 peak
PVC	230–580	2 peak

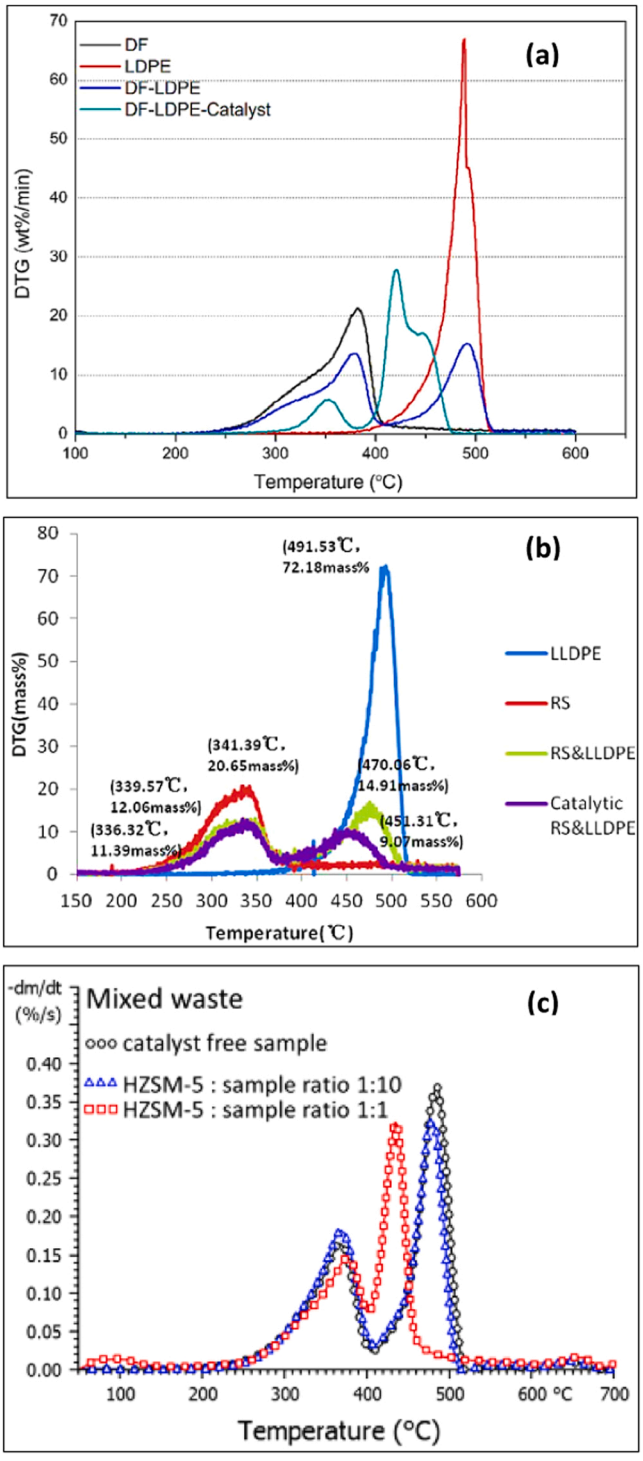

Fig. 1. Co-pyrolysis of (a) Doughlas fir saw dust and LDPE w/ and w/o ZSM-5 [33] (b) Rice straw and LLDPE w/ and w/o Co/ZSM-5 [34] (c) biomass mixture (pine saw dust, news paper, cardboard) and plastic mixture (PE, PP, PET) w/ and w/o HZSM-5 [35].

higher temperature compared to the DTG curve of individual biomass or plastic sample depending upon the type of biomass-plastic blend, blend ratio, and heating rate (see Table S3). In ZSM-5 catalyzed co-pyrolysis (i.e., Fig. 1(a)), two peaks were observed for Doughlas-fir and LDPE decomposition, respectively, at a lower temperature compared to non-catalytic co-pyrolysis. This indicated the significant impact and benefit during catalytic decomposition of the blend. The shift in the LDPE decomposition peak remained more prominent. Similar behavior was observed for Co/ZSM-5 catalyzed co-pyrolysis of rice straw and LLDPE (Fig. 1(b)), and HZSM-5 catalyzed co-pyrolysis of biomass mixture (pine sawdust, newspaper, and cardboard) and plastic mixture (PE, PP, and PET) (Fig. 1(c)).

The DTG curves of pine powder (B) and LDPE (P) co-pyrolysis indicated for without catalyst (BP), Ni-impregnated biomass (BP-Ni), Ni-modified/HZSM-5 catalyzed (BP@Ni/HZ), and Ni-impregnated biomass with HZSM-5 catalyzed (BP-Ni@HZSM-5) (Fig. 2). In BP-Ni and BP@Ni/HZ, two peaks were observed for pine and LDPE, respectively, at lower temperatures compared to BP. However, for BP-Ni@HZSM-5, only one peak was observed for pine decomposition. The absence of a second peak in the case of BP-Ni@HZSM-5 suggested a negligible impact of Ni-impregnated biomass with HZSM-5 catalysis on LDPE decomposition. However, Ni-impregnation without HZSM-5 catalysis (BP-Ni) affected pine and LDPE decomposition but resulted in more char and non-condensable gases. Therefore, TGA results suggest that co-pyrolysis reactor can be operated at moderate temperature (below 600 °C) and use of suitable catalyst further impacted in lowering the decomposition temperature of the blend compared to non-catalytic co-pyrolysis.

The effect of heating rate on blends co-pyrolysis can be described from Table S3 (Supporting information). Increase in heating rate at 25 wt% LLDPE blending with Bamboo saw dust, decomposition temperature range and DTG peak shifted to higher temperature for both phase-I and phase-II [85]. Similar trend found across different wt% blending of LLDPE with Bamboo saw dust [85] and blending of PET with Samanea saman seeds [97]. Uniform temperature across the solid mass could be achieved at a lower heating rate as an enough time was available for heating, but it could enhance the char formation via secondary reactions and more thermal cracking of pyrolysis volatiles into non-condensable gases. Whereas, at the higher heating rates, a temperature gradient across the solid mass could be responsible for this temperature shift [30], but increase in rate of decomposition with the heating rate observed because of higher thermal energy at higher heating rate [31] and the secondary reactions might change with the heating rate [32]. Therefore, TGA results suggest that higher heating rate with low residence time of volatiles is desirable in fast co-pyrolysis reactor to produce high yield of bio-oil. A reactor configuration should be such that rapid uniform heating of blend can be easily achieved at higher heating rate.

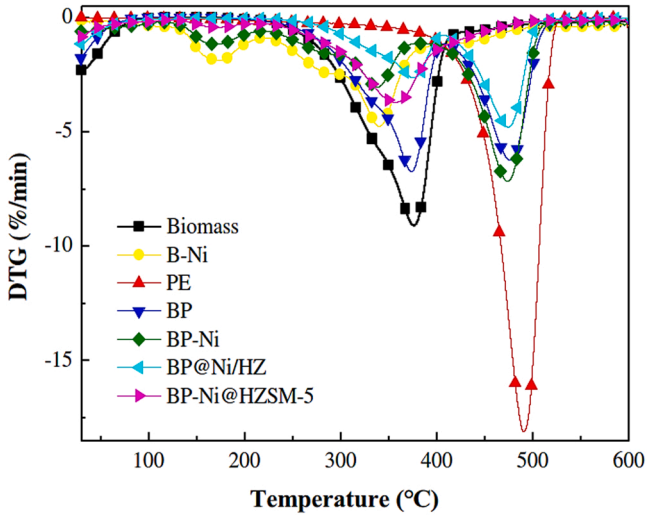

Fig. 2. DTG curve of co-pyrolysis of pine powder (B) and LDPE (P) without catalyst (BP), after Ni-impregnated biomass (BP-Ni), Ni-modified/HZSM-5 catalyzed (BP@Ni/HZ) and Ni-impregnated biomass with HZSM-5 catalyzed (BP-Ni@HZSM-5) [B to P ratio = 1:1, catalyst to blend = 2:1] [36].

2.1.2. Relation between reactivity and synergistic effects in TGA

TGA information of co-pyrolysis is reviewed and tabulated (Table S3) to correlate the reactivity and synergistic effect of blends (or reactants). Reactivity (R_M) in wt% min^{-1} °C can be calculated using Eq. (1) [37].

$$R_M = 100\left(\frac{DR_{max}}{DTG\ peak}\right) \quad (1)$$

where DTG peak is peak temperature (°C), DR_{max} is maximum decomposition rate at DTG peak (% min^{-1}). The synergistic effect is determined in the TGA study as the difference in the experimental and theoretical (or calculated) value of weight loss in wt%, i.e., ΔW (convention adopted here that +ve value → synergistic effect and −ve value → anti-synergic effect). For example, in the study of Alam et al. [38] $R_M = 100 \times \left(\frac{1.68}{309} + \frac{3.12}{449}\right) = 1.24$ wt% min^{-1} °C^{-1} for the 25% blend at the heating rate of 5 °C min^{-1} was obtained.

TGA analysis of co-pyrolysis of bamboo sawdust and LLDPE at different blend and heating rate was carried out [38]. From Table S3 (Supporting information), with %LLDPE increase from 25 to 75 wt% in the blend, DR_{max} in Phase-I decreased, while DR_{max} in Phase-II increased at all the heating rates. In Phase-I (i.e., 180–400 °C), the decomposition of cellulose and hemicellulose occurred and was slightly affected by the presence of LLDPE. Phase-I peaked around 310–340 °C; LLDPE softened to the plastic state, which covered biomass particles and inhibited the evolution of volatile matter at this Phase-I. In Phase-II (i.e., 360–540 °C), the decomposition of LLDPE dominated, and also the free radicals produced from LLDPE helped in the decomposition of lignin. A similar result was evident in the co-pyrolysis of rice straw-HDPE [39]. corn stalk-HDPE [40], and Samanea saman seeds-PET [29], as shown in Table S3.

From Table S3, it is evident that higher reactivity resulted in a higher synergistic effect at 75 wt% LLDPE blend for all the heating rates studied [38]. Lower activation energy was also reported at 75 wt% LLDPE blend. A similar result was evident at 80 wt% HDPE blend with rice straw [39] and at 50 wt% HDPE blend with corn stalk [40], as shown in Table 4. Anti-synergistic effects were observed in all the blends of Samanea saman seeds with PET at a different heating rate [29]. However, at 25 wt% and 50 wt% PET blends, the reactivity of co-pyrolysis remained almost equally high, and low anti-synergistic effects were evident in these blends. The 25 wt% PET blend was reported to be suitable for pyrolysis with a significantly high yield of 54.24 wt% and good quality fuel in lower moisture and carbon content, lower viscosity, and higher heating value. The lower activation energy was evident in the 25 wt% PET blend, which resulted in high reactivity and bio-oil yield. Therefore, it can be inferred that high reactivity resulted in a high synergistic effect in TGA analysis. This needed to be verified in the reactors like a fixed-bed, fluidized-bed, ablative, rotating cone, etc. In a reactor, where a large amount of feedstock is processed, the triple-phase interaction (i.e., solid-liquid-gas) differed from the triple-phase interaction in TGA, where a small quantity (usually 5–10 mg) was used. Volatiles evolved in the more in-depth section of the reactor spend more time to react with solid biomass and melt (liquid) while passing through them. Therefore, one has to explore the possibility of the correlation between reactivity (R_M) obtained from TGA and yield and quality of bio-oil from co-pyrolysis of blends and their synergistic effects in various co-pyrolysis reactors.

2.2. Yield and quality of bio-oil and synergistic effects in various co-pyrolysis reactors

The co-pyrolysis results of different biomass/plastic blends in the various reactors presented in Table 2 were used to explore the relation between R_M and yield and quality of bio-oil. In co-pyrolysis reactors, the synergistic effect was determined as a difference in the experimental and theoretical value of bio-oil yield (in wt%) from co-pyrolysis of blends. H/C and O/C molar ratios can be used as indicative tools for the quality of bio-oil (Table 3). Bio-oil with a high O/C molar ratio comprises higher amounts of oxygenated compounds, making the quality of bio-oil unsuitable as liquid transportation fuel or direct combustion into engines. The R_M and a synergistic effect was calculated from TGA information and bio-oil yield, respectively, if not reported in the original published report (Table 2).

Pinewood co-pyrolyzed with PE and PVC at different proportions (viz. 25, 50, and 75 wt% polymers) and 600 °C in a fixed bed reactor [41]. The R_M values for PE were 0.48, 0.51, and 0.52 and for PVC were 0.66, 0.64, and 0.57 at 25, 50, 75% polymer, respectively. High bio-oil yield of 53 wt% and synergistic effect of +2.28 wt% observed, corresponding to the high R_M value at 75 wt% PE. Bio-oil quality improved as the H/C ratio increased from 1.3 (Pinewood bio-oil) to 1.83, and the O/C ratio reduced from 0.15 (Pinewood bio-oil) to 0.018. In PVC case, the bio-oil yield obtained from all the blend ratios was anti-synergistic. However, the high bio-oil yield of 17.5 wt% and least anti-synergistic effect of −1.87 wt% corresponded to high R_M value at 25 wt% PVC. Though the addition of PVC deteriorated the quality of bio-oil, the better quality was obtained at 25 wt% PVC compared to other blend ratios. Furthermore, at 75 wt% PE and 25 wt% PVC blends with pinewood, the lowest activation energies of 78.1 kJ mol^{-1} and 134.6 kJ mol^{-1}, respectively, were reported.

Beechwood co-pyrolyzed with PE at different proportions (viz. 40 wt % and 60 wt% polymers) and 650 °C in a fixed bed reactor [42]. Though 60 wt% PE blend resulted in an anti-synergistic effect, the high bio-oil yield (50.3 wt%) obtained corresponding to the high R_M value (9.04 wt% min^{-1} $°C^{-1}$). Furthermore, bio-oil quality improved as oxygenated compounds of bio-oil reduced from 10.4 wt% (beech wood bio-oil) to 4.9 wt%.

Neem seeds co-pyrolyzed with waste nitrile gloves (WNG) at different proportions (viz. 16.67, 25, and 50 wt% WNG) and 400–600 °C temperature with and without CaO and Al_2O_3 in a fixed bed reactor [43]. At 500 °C and 80 °C min^{-1}, bio-oil yield (43.52 wt%) and the synergistic effect remained high corresponding to the high R_M value (2.37 wt% min^{-1} $°C^{-1}$) at 25 wt% WNG in non-catalyzed co-pyrolysis compared to CaO and Al_2O_3 catalyzed co-pyrolysis. Furthermore, adding waste nitrile gloves in neem seeds improved the quality of bio-oil obtained from the non-catalyzed process as O/C reduced to 0.133 and heating value increased up to 34.15 MJ kg^{-1} compared to 0.46 O/C ratio and 23.19 MJ kg^{-1} heating value of bio-oil from neem seeds. However, higher quality of bio-oil obtained from the catalyzed process as O/C reduced to 0.064 and 0.056 and consequently heating value increased up to 40.36 and 39.21 MJ kg^{-1} with CaO and Al_2O_3, respectively. Therefore, though high yield corresponded to high R_M in the non-catalytic process, a better quality of bio-oil with relatively less yield could be achieved in the catalytic process. Pinewood sawdust (PSD) was co-pyrolyzed with waste tyre (WT) at different proportions (viz. 25%, 50%, and 75% WT) and 500 °C in a conical spouted fluidized bed reactor (CSBR) [44]. The bio-oil yield obtained from all the blend ratios was anti-synergistic. However, the high bio-oil yield (67 wt%) and least anti-synergistic effect (−1.2 wt%) corresponded to the high R_M value (4.07 wt% min^{-1} $°C^{-1}$) at 25% WT.

From our analysis of published data of co-pyrolysis of biomass and polymer blend in different reactors, we found that yield and quality of bio-oil can directly correspond to the R_M value determined from TGA, but no clear relation was observed between R_M and synergistic effect of biomass/plastic blends. The information remained inadequate to explore the relationship between activation energy and R_M. A large volume of literature on the co-pyrolysis of biomass and polymer blend was unable to thoroughly explore the interaction between the two reactants during the process, except for a few TGA studies of biomass/plastic blends. Therefore, it will be useful and insightful to couple TGA studies with the co-pyrolysis process in any reactor. The TGA information in terms of reactivity and synergistic effects discussed in this section enable researchers to understand the effect of process parameters variations on the yield and quality of bio-oil, and thus it is recommended prior to going for bio-oil production in a co-pyrolysis reactor.

3. Synergistic effect of biomass and plastic co-pyrolysis

The lignocellulosic biomass consists of C—H, C—O, C—C, and O—H bonds coupled with aromatic ring oxygenates that form cellulose, hemicellulose, and lignin [46]. A minor percentage of inorganics (Ca, Mg, Na, K) also found in the biomass. In contrast, plastics are mainly hydrocarbons containing linear and aromatic polymers. It includes an excellent hydrogen-to-carbon ratio (H/C) compared to biomass, improving bio-oil quality. The plastics, through hydrogen donation, promote the hydrodeoxygenation of biomass-derived oxygenated compounds during co-pyrolysis [47–49]. The synergistic effect of biomass and plastics governs the co-pyrolysis final product distribution, including bio-oil quality, and remains key for waste-to-energy conversion techniques. The interaction of biomass compounds (viz. cellulose, hemicellulose, and lignin) with plastic remain crucial to recognize the nature of the biomass/plastic co-pyrolysis system and hence critically discussed in this section.

The co-pyrolysis of cellulose with polyethylene (PE) at 600 °C produced aliphatic hydrocarbons (from PE) and levoglucosan (from cellulose) rich bio-oil along with pyrans, aliphatic ketones, and higher acetic acids [16]. The yield of acetic acid increased during co-pyrolysis due to the interaction of C_1 – C_4 hydrocarbons (derived from PE) with cellulose-derived oxygenated compounds. Upon increasing the pyrolysis time, the ketone formation (i.e., 2-hexanone, 2-oxanone, 2-nonanone, and 2-dodecanone) increased, whereas aldehydes decreased due to the interaction between PE derive hydrocarbon chains and aldehydes (i.e., acetaldehyde) as demonstrated in the Fig. 3[A] [50].

The cellulose, when co-pyrolyzed with PP in different proportions, over 500–800 °C, in a Pyroprobe® reactor, produced high-quality bio-oil [51]. The interaction of cellulose with PP resulted in the increased formation of C_8 – C_{20} long-chain alcohols and hydrocarbons, while it suppressed furans, anhydrosugars, and aldehydes/ketones production at the same time (Fig. 3[B]). The cellulose to PP ratio of 25: 75 governed the alcohol and hydrocarbons (aliphatic and aromatic) formation, with the maximum yields of 36 wt% alcohols and 45 wt% hydrocarbons, at 600 °C. Further, the interaction of cellulose with polypropylene (PP) promoted the hydroxyl, hydrogen, and methyl abstraction reactions during the co-pyrolysis process.

The polystyrene (PS) and cellulose interaction increased the bio-oil yield and quality (i.e., decreases in pour point, density, and acid number) than bio-oil derived from the individual feedstock [52]. A reduction in cellulose to PS ratio increased the formation of hydrocarbons within bio-oil or vice versa. The co-pyrolysis of pine cone (*Pinus pinea* L.) and cellulose with synthetic polymers (PP, PE, and PS) at 500 °C revealed an enhanced yield and composition of bio-oil compared to pyrolysis of individual feedstock [53] (Fig. 3[C]). The PP, PE, and PS added to pine cone or cellulose provided in-situ hydrogen during co-pyrolysis and thus increased the bio-oil yields. Further, the char derived after co-pyrolysis contained more calorific value than the char obtained through biomass pyrolysis alone.

The interactions of cellulose-derived compounds with PS, PP, and PE, and polyethylene terephthalate (PET), over 450–600 °C, in a Py-GC × GC/MS (pyrolysis–gas chromatography–mass spectrometry) system suggested the notable interpretations [15]. The PS-cellulose co-pyrolytic environment promoted intra-and-intermolecular hydrogen transfer,

Table 2
Relation between RM and yield and quality of bio-oil from co-pyrolysis reactor.

Reactor configuration	Solid type	wt%[$]	DTG peak (in °C) [DRmax in % min^{-1}]	R_M (wt% min^{-1} $°C^{-1}$)	Ea (kJ mol^{-1})	Dry mass H/C molar ratio	Dry mass O/C molar ratio	Yield (wt%) Biooil-Char-Gas [ΔW (wt %)][a]		Biooil H/C molar ratio	Biooil O/C molar Ratio	Other results
PW (Pine Wood) + PE, PVC [Fixed Bed Reactor: 600 °C, Run 15 min, N_2 150 mL min^{-1}, 5 g sample & **TGA**@10 °C min^{-1}]								**Ref.** [41]				
Horizontal [Quartz tube L 50 cm, ID 3.5 cm]	PW [48.9/ 16.8/ 29.8][b,#]		350 [1.5]	0.43	88.1	1.38	0.64	19.1-20.1-60.8		1.3	0.15	
	PE		465 [2.7]	0.58	220.6	2	0	61-0-40		1.87	0	
	PVC		287 [1.8] 459 [0.4]	0.71	186	1.48	0	18.1-7.9-74		0.82	0	
	PW + PE	75	350 465	0.52 [highest]	78.1 [lowest]	1.94	0.10	53-3.9-33.1 (+2.28/ −1.12)[a] Synergistic		1.83	0.018	81.6% mono-aromatics of Total Aromatics
	PW + PVC	25	303 442	0.66 [highest]	134.6 [lowest]	1.40	0.50	17.5-20-62.5 (−1.87/ +2.9)[a] Anti-synergistic		0.86	0.077	Only 6.6% mono-aromatics
BW (Beech Wood) + PE [Fixed Bed Reactor: 650 °C, 10 °C min^{-1}, He 100 mL min^{-1} & **TGA**@10 °C min^{-1}]								**Ref.** [42]				
Horizontal	BW [41.6/ 26.5/ 23.1][b]		353[15]	4.25	NA	1.49	0.66	10.4-17.6-10.8				10.4% oxygenates
	PE		478[27]	5.64	NA	2.0	0	83.1-0-2.1				No oxygenates
	BW+PE	40	353[15] 480[22]	8.83	NA	1.76	0.31	43.5-10.8-6.3 (+4.02/ +0.24) Synergistic				7.2% oxygenates
	BW+PE	60	353[15] 482[23]	9.02	NA	1.86	0.18	50.3-7.3-4.6 (−3.72/ +0.26) Anti-synergistic				4.9% oxygenates
NM (Neem Seeds) + WNG (Waste Nitrile Gloves) with and without CaO, Al_2O_3 [Fixed Bed Reactor: 400–600 °C, 50–100 °C min^{-1}, N_2 80 mL min^{-1} & **TGA**@10 °C min^{-1}]								**Ref.** [43]				
Vertical	NM [40.04/ 22.94/ 10.58]		357[16]	4.48	NA	1.72	0.54	– LHV[c]: 23.19		2.1	0.46	Ar./Par./Ole. (vol %)[d] 11.34/ 83.87/4.93 Iso-paraffins index 0.27
	WNG		465[19]	4.08	NA	1.31	0.092	–				
	NM + WNG	16.67			NA	1.62	0.434	– (ΔW < 0) Anti-synergistic				
		25	335[5] 455[4]	2.37	NA	1.58	0.39	43.52-24-32.55 (ΔW > 0)[e] Synergistic HV: 34.15	500 °C, 80 °C min^{-1}	1.14	0.133	Ar./Par./Ole. (vol%) 25.78/52.05/ 22.49 Iso-paraffins index 3.15
		50			NA	1.47	0.27	– (ΔW < 0) Anti-synergistic				
	NM + WNG + CaO (17 wt% CaO)	25	342 [4.5] 456[3]	1.97	NA	1.58	0.39	40.42-28-32 (ΔW > 0) Synergistic HV[b]: 40.36	500 °C, 80 °C min^{-1}	1.04	0.064	Ar./Par./Ole. (vol%) 26.62/70.04/ 3.65 Iso-paraffins index 1.94
	NM + WNG + Al_2O_3 (17 wt% Al_2O_3)	25	350[4] 457[3]	1.80	NA	1.58	0.39	37.14-31-31 (ΔW > 0) Synergistic HV: 39.21	500 °C, 80 °C min^{-1}	1.01	0.056	Ar./Par./Ole. (vol%) 17.06/29.94/ 53.47 Iso-paraffins index 2.10
PSD (Pine Wood Saw Dust) + Waste tyre (WT) [CSBR: 500 °C, Run 30 min, N_2 8 L min^{-1} (1.5 times minimum spouting velocity), 1 g min^{-1}, Bed 150 g silica sand, & **TGA** @ 15 °C min^{-1}] [10^3–10^4 °C s^{-1}, VRT: 30 ms in spout zone & 500 ms in annulus]								**Ref.** [44]				
	PSD			3.65	NA	1.47	0.68			2.44	0.89	

(*continued on next page*)

Table 2 (*continued*)

Reactor configuration	Solid type	wt%[$]	DTG peak (in °C) [DRmax in % min^{-1}]	R_M (wt% min^{-1} $°C^{-1}$)	Ea (kJ mol^{-1})	Dry mass H/C molar ratio	Dry mass O/C molar ratio	Yield (wt%) Biooil-Char-Gas [ΔW (wt %)][a]	Biooil H/C molar ratio	Biooil O/C molar Ratio	Other results
Vertical [plant scale]			370 [13.5]					71.6-18.1-10.3 HHV: 19.5			n.d HCs 45.1% oxygenates
	WT		380 [9.0] 430 [7.75]	4.17	NA	1.09	0.042	55.2-35.9-9.1 HHV: 41.9	1.42	0.02	51.5 HCs 7.3% oxygenates
	PSD + WT	25	372[13] 435 [2.5]	4.07	NA	1.33	0.45	67-23-10 (−1.2/+0.5) Anti-synergistic			
		50	372 [11.5] 435 [3.9]	3.99	NA	1.24	0.28	62-28-10 (−1.7/+1) Anti-synergistic HHV: 28.9	1.72	0.35	20.3% HCs 33.4% oxygenates
		75	375 [10.5] 435 [4.5]	3.83	NA	1.15	0.15	58-33-9 (−1.5/+1.6) Anti-synergistic			

VRT: Volatiles residence times.
NA: Not available
[$] wt% polymer in blend.
[#] From Sharypov et al. [45].
[a] Difference in experimental & theoretical value of yield of bio-oil/char in wt% (+ve means synergistic effect).
[b] Cellulose/hemi-cellulose/lignin.
[c] LHV/HV/HHV: Low heating value or heating value or high heating value in MJ kg^{-1}.
[d] Aromatics/paraffins/olefins.
[e] ΔW = Difference in experimental and theoretical yield of bio-oil based on TGA analysis and not from fixed bed reactor scale yield.

Table 3
Bio-oil quality.

H/C molar ratio	O/C molar ratio	Bio-oil quality
High	High	Oxygenates
High	Low	Paraffins and/or Naphthenes
Low	High	Oxygenates
Low	Low	Aromatics and/or olefins

leading to ethylbenzene formation [54]. However, the detailed mechanisms of hydrogen transfer from PS or cellulose remained unclear in such studies. The pyrolytic environment of cellulose, PP, and PS favored alkylated benzene generation due to the interactions of PP-derived aliphatic hydrocarbons and PS-derived aromatics. The comparison of ethylbenzene yield from cellulose/PS and cellulose/PP/PS pyrolysis suggested that the addition of PP encouraged the ethylbenzene and other single-ring aromatic compound formations. The cellulose/PP/PS co-pyrolysis generated smaller yields of furans and pyrans and higher yields of styrene/styrene oligomers, compared to cellulose/PS co-pyrolysis. This suggested that the interactions between PS and PP promoted alkylated benzene generation, while the addition of PP suppressed furans and pyrans formations up to some extent. For co-pyrolysis of cellulose with PE/PET, PP, or PS, the alkylated benzenes formation suppressed and single as well as more-ring aromatic products increased; however, the detailed insight of such reduction of alkylated benzenes and aromatic compounds remained unclear in the literature. We suggest that the aromaticity in the product mixture increased due to the positive contribution of PET-derived aromatics during the co-pyrolysis.

For the PE and raw biomass such as beech wood co-pyrolysis, PE was melted instantly under pyrolytic conditions (≈ 650 °C), enabling the dispersion of beech wood in it. Eventually, it promoted the ejection of beech wood's cellulose-, hemicellulose-, and lignin-derived pyrolysates [55]. These pyrolysates interacted with each other before coming in contact with PE pyrolysates, possibly because of beech wood's microscopic cell wall structure. The mixing of cellulose pyrolysates with PE increased the yields of non-condensable gases while suppressed the char formation and enhanced the yield of bio-oil possibly due to C—C bond repolymerization and lignin coupling reaction [56,57].

Another report discussed the interactions of low-density polyethylene (LDPE) with sunflower stalk, cedarwood, and Fallopia Japonica Stem (FJS) in the context of increased yield and composition of bio-oil [58]. The decomposition of biomass and LDPE compensated for each other because the inorganic biomass contents promoted LDPE breaking. The synergistic effect found to be encouraging for aliphatic products within bio-oil; however, oxygenated and phenolic compounds (acids, ethers, aldehydes, ketones, furans, ketones, sugars, and phenols and sugars) remained suppressed within bio-oil. Further, a significant percentage of alcohol was observed within biomass/LDPE derived bio-oil, possibly because the OH radicals eliminated from the biomass combined with the LDPE derived aliphatic compounds eventually resulted in a higher alcohol yield. The synergistic effect of biomass and plastic on aromatic compounds' production remained dependent on biomass feedstock. cedarwood and sunflower stalk interaction with LDPE increased aromatic compounds, while the FJS/LDPE mixture showed an opposite trend. The co-pyrolysis of PP with corn cob at 320 °C suggested that for biomass-rich system (i.e., PP < 50 wt%), the feed particle experienced shrinkage well before the melting PP (≈ 130 °C) and hence did not interacted significantly with PP [59]. In contrast, for PP-rich co-pyrolysis, the corn cob particle faced expansion because of the hydrogen bonding between plastic compounds and the biomass phenolic moieties.

Thus, the synergistic information of biomass and plastic could be crucial to correlate the final pyrolysis product distribution with the feedstock composition. It sheds light on the possible pyrolysis reactions amongst the biomass and plastic-derived compounds (concerning operating conditions), which eventually governed bio-oil quality (or composition). However, the quality of bio-oil derived from biomass/plastic co-pyrolysis can be enhanced by incorporating a suitable catalyst.

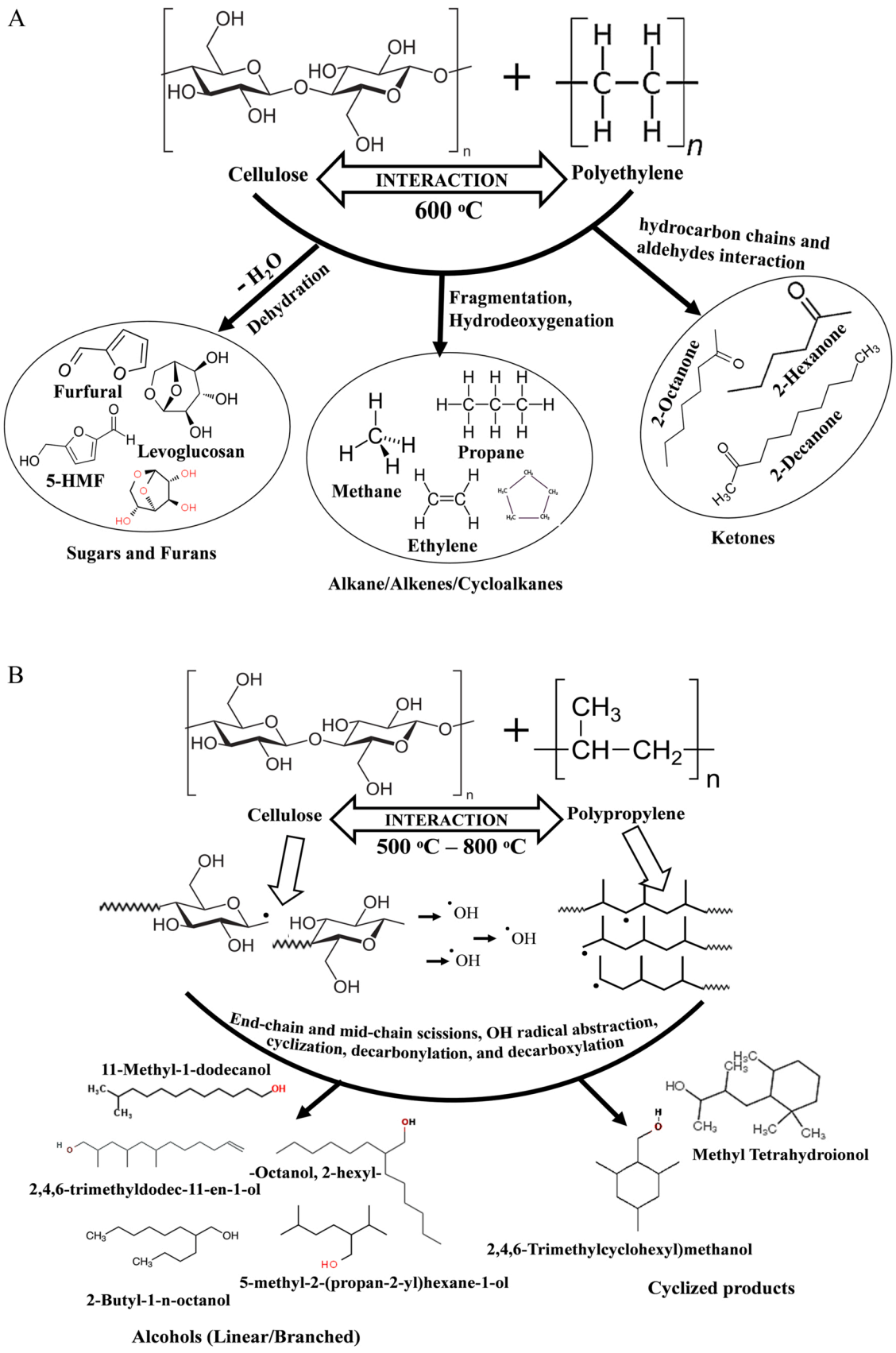

Fig. 3. [A] Cellulose and PE interactions forming sugars, furans, alkanes, alkenes, and ketones [16] [B]: Cellulose and PP interactions forming alcohols and cyclization products [51] [C]: Cellulose and PS interactions forming 1-ring, 2-ring aromatics and olefins [15,52].

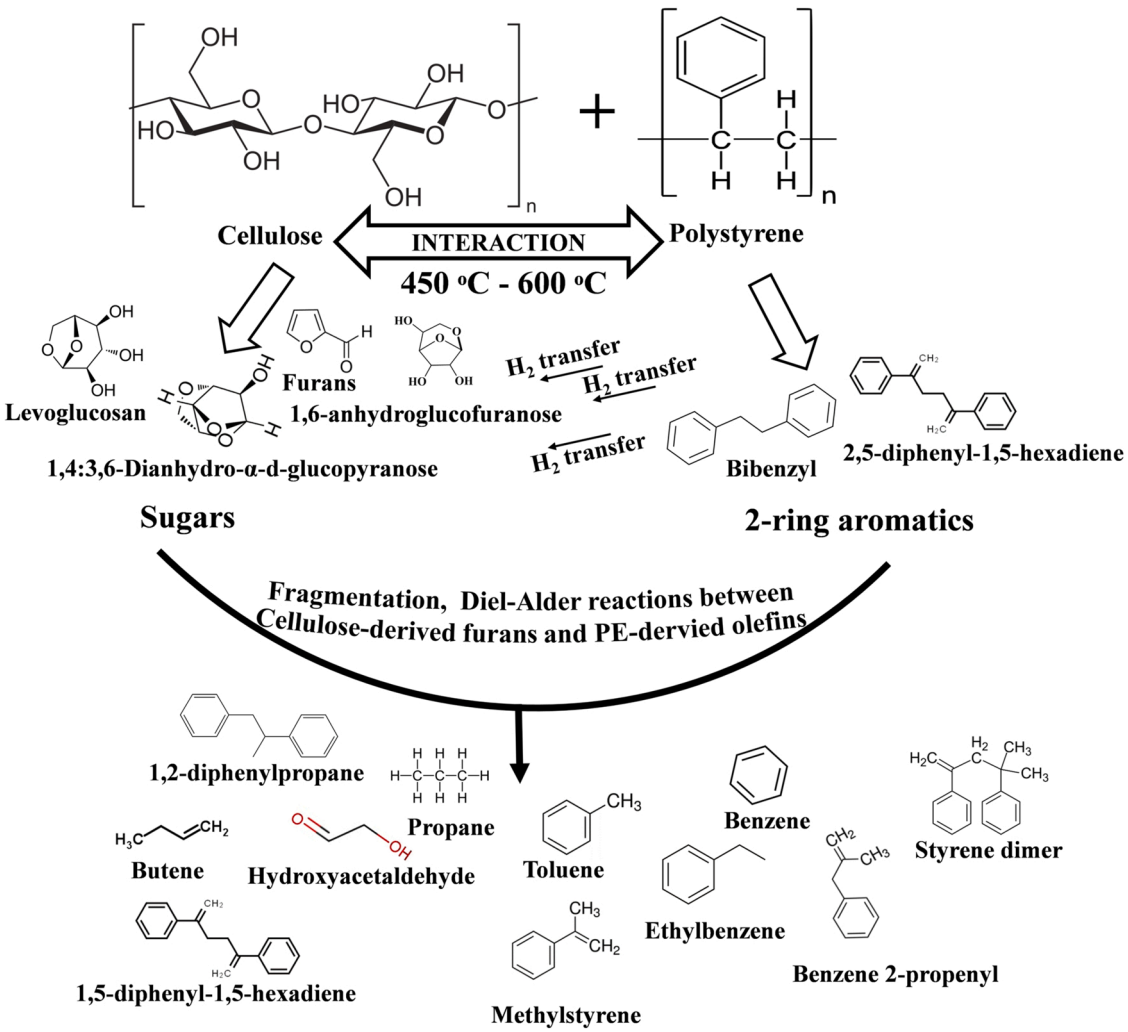

Fig. 3. (*continued*).

In such cases, the synergistic effect of biomass and plastics-derived compounds over the catalyst surface determines the final composition of bio-oil. Hence, the in following section discussion on the synergistic effect of biomass and plastic-originated compounds under the catalytic environment is presented.

4. Use of catalysts in co-pyrolysis

The use of catalysts during co-pyrolysis allowed the selective formation of desired compounds within the product mixture, especially forming bio-oil. Various catalysts such as metal oxides, spent FCC, alumina, CeO_2, and zeolites have been used for biomass and plastic co-pyrolysis. Each of these catalysts is discussed in brief in the following sections. The information regarding catalyst, pyrolysis conditions, and key results is summarized in Table 4.

Table 4
Catalysts for co-pyrolysis of biomass and plastic.

Catalyst	Feed	Reactor type	Pyrolysis conditions		Product yield	Key results	Ref.
			Biomass to plastic ratio	Temp,°C			
LOSA-1, Spent FCC, γ-Al_2O_3	Blacl-liquor lignin + PE/PP/PS	Fluidized bed reactor	1:1	450–650 °C	55.3%	Aromatic and olefin yield increased with PE proportion	[72]
HZSM-5, CaO	Hemicellulose + LLDPE	Duel bed CFP	1:1	450–700 °C	40%	Increased aromatic yield	[74]
P/Ni/ZSM-5	Pine wood + LDPE	Semi-batch reactor	1:0, 4:1, 2:1, 1:1, 0:1	550 °C	~ 40%	Increased carbon yield	[75]
Spent FCC	Groundnut shell + PP/PS	Semi-batch reactor	1:2, 1:1, 2:1	510 °C	Oil ~ 73%	The increase in plastic proportion in the feed enhanced the liquid yield.	[81]
ZnO, CaO, Fe_2O_3, MgO	Poplar wood + PP	Py-GC/MS	1:1	600 °C	–	Lower carboxylic acid yield and improved alkene yield	[82]
CeO, HZSM-5	Corn stover + LDPE	Tandem catalytic bed pyrolyzer	total weight of sample was 0.5 g	600 °C	85%	H/C ratio of 0.7	[83]

4.1. Spent FCC

Spent FCC catalyst with varying Si/Al ratios is effectively used for the co-pyrolysis of biomass and plastic [1a]. The catalyst can directly be used without any pre-treatment. Spent FCC catalysts and other large pore-size zeolites are better catalysts for producing liquid hydrocarbons during co-pyrolysis. Spent zeolite catalyst as a waste of FCC unit is cheap [54].

4.2. Metal oxides

Metal oxides such as CaO, CuO, ZnO, Fe_2O_3, Al_2O_3, MgO, SiO_2 are economical and accessible catalysts. Also, they are found to be effective in the removal of oxygen from co-pyrolysis products. A lower carboxylic acid yield and increased alkene yield were observed in the case of metal oxides when poplar wood and polypropylene mixture was co-pyrolyzed in a reactor at 600 °C. Compared with non-catalytic pyrolysis, the ketone formation has been improved in the presence of ZnO, CaO, and MgO [59]. Catalytic co-pyrolysis of black-liquor lignin with PE/PP/PS yielded higher selectivity for naphthalene and its derivative in the presence of Al_2O_3 as a catalyst [54]. Compared to zeolites that suppress oil products' yield, mesoporous SiO_2-Al_2O_3 are interesting options to increase liquid product yield.

4.3. Zeolites

The zeolite-type catalysts were preferred for co-pyrolysis of biomass and plastics because of their large surface area, high thermal stability, and abundant acid sites, making them suitable for cracking and dehydration [60]. Notably, the reactions involved in co-pyrolysis remained sensitive to acidity, porosity, pore size, and crystallinity of zeolite, which can be tuned as per the process demand. On the contrary, it is noteworthy that zeolites also promoted the formation of gaseous products and bio-char while suppressing the yield of liquid products in some cases of co-pyrolysis [61]. One possible reason for such behavior could be attributed to the cracking of hydrocarbon vapors in the presence of zeolites. Interestingly, zeolites with 5.2–5.9 Å and large size pores can promote the formation of aromatic compounds. The aromatic yield order remained as ZSM-5 > beta zeolite > mordenite > Y-zeolite among the various zeolites. Zeolites deactivate rapidly by coking due to their surface acidity and pore structure. The effectiveness of zeolite catalysts was gauged mainly from high aromatic products and less coke formation. One possible reason for higher aromatics yield in the presence of dedicated ZSM-5 could be its improved stability against coke formation and improved mass transport of reaction intermediates [62].

In particular, the co-pyrolysis of cellulose with LDPE over ZSM-5 predominantly produced a higher yield of aromatic compounds than the individual pyrolysis, indicating the synergy between the two reactants on the catalyst surface. Diels–Alder reactions of the cellulose-derived furanic compounds (i.e., furfural) with the LDPE-derived olefins (i.e., ethylene and propylene) over ZSM-5 catalyst resulted in the aromatics formation (e.g., toluene and xylenes) [63,64]. LDPE-derived hydrocarbons also provided hydrogen to the oxygenated compounds of cellulose and helped to reduce coke on the catalyst surface. Further, the cellulose interaction with PP produced a lower yield of aromatics than the former because PP-derived branched olefins were unable to react with the cellulose-derived furans due to steric hindrance and electronic effects branching.

The PS and cellulose co-pyrolysis on ZSM-5 did not show much interaction as the styrene derived from PS remained poor dienophile species for Diels–Alder reactions with cellulose-derived furans [65]. The PS-derived styrene as an intermediate further alkylated with allene of the furans and resulted in indene formation under the ZSM-5 environment. The indene so formed further reacted with allene and generated naphthalene as a final product [63]. The pyrolytic reactions of pinewood sawdust and LDPE over the ZSM-5 surface resulted in lower yields of aromatic/aliphatic hydrocarbons and coke as the biomass material produced more oxygenated products from the depolymerization of hemicellulose and lignin, in addition to cellulose.

Alkali lignin when co-pyrolyzed with PP over ZSM-5 catalyst under (ex-situ mode) unconventional microwave heating, produced alkanes, alkenes, aromatics, and cycloalkanes as the products [66]. Upon increasing catalyst to feed ratio, the formation of aromatics enhanced, while the cycloalkanes yields suppressed simultaneously. The lignin-derived oxygenates over ZSM-5 catalyst converted into aromatics and alkenes. The alkenes, after hydrogenation, further converted into alkanes, although the yield of alkanes was found lower than the rest of the products. The vapors of lignin and plastic (PP) co-pyrolysis on the ZSM-5 surface underwent cracking reactions. At the same time, the hydrogen transfer from PP-derived compounds to the lignin oxygenates produced the alkenes, which further experienced Diels–Alder reaction, aromatization, and cyclization reactions to result in aromatics and cycloalkanes formation.

The zeolites, particularly ZSM-5, were preferred because of their ability to selectively convert the oxygenated volatile products of pyrolysis into hydrocarbon-rich aromatic compounds [67]. The biomass-derived volatiles over the active sites of HZSM-5 converted into aromatics (BTX) and olefins through multiple reactions, including depolymerization, decarbonylation, decarboxylation, oligomerization, dehydration, isomerization, and aromatization. The higher yield of xylene suggested the dominant nature of Diels–Alder reaction between furans (i.e., 5-HMF) and PE-derived olefins. The cellulose-derived anhydrosugar compound (or levoglucosan) dehydrated into furan and light oxygenates as it could not reach the active sites of HZSM-5 due to its large molecular size [68]. The olefins obtained primarily from the PE during co-pyrolysis, which further underwent Diels–Alder and dehydration reactions with furan and furfurals (at Brönsted acid sites) and formed BTX [69].

Similarly, other zeolites such as H-beta catalysts have also been reported effective in co-pyrolysis because of their strong acidity and appropriate pore size. The use of H-beta zeolite facilitates co-pyrolysis of Cork-Oak (CoOak) and waste plastic film (WPF) mixture due to strong acidity and appropriate pore size [70]. Similarly, HZSM-5 and mesoporous Al-MCM-41 produced aromatic hydrocarbon compounds in co-pyrolysis of torrified yellow poplar with HDPE (high density polyethylene) because of their acidity and organized pore structure [71]. In a further study, the co-feeding of black-liquor lignin with PE, PP, and PS improved the liquid (or bio-oil) yield [72]. In this regard, the catalysts' activity followed the order LOSA-1 (majorly ZSM-5) > spent FCC (fluidized cracking catalyst) > Gamma-Al_2O_3 > sand. The co-pyrolysis of black-liquor lignin with PE produced more benzene, naphthalene, and its derivatives. In contrast, lignin co-pyrolysis with PS generated more styrene.

4.4. Metal impregnated zeolites

Doping of metals can significantly improve the texture, acidity, and porosity of zeolites. The metal impregnation helps in tuning the activity of the zeolite for the selective formation of targeted products. A series of phosphorous (P) and phosphorous-nickel (P/Ni) modified zeolites were tested for pinewood and low-density polyethylene (LDPE) co-pyrolysis. As a result, an increase in olefins and aromatic hydrocarbons yield to 52.8% and 54.1% in the presence of phosphorous and phosphorous-nickel catalysts, respectively, have been measured compared to 42.9% oil yield without these metal loadings [44].

4.5. Dual catalytic systems

As discussed earlier, ZSM5 is the most preferred catalyst for pyrolysis due to its structure and medium pore size. This puts limitation on the transport of bulky molecules during the biomass and plastic co-pyrolysis when ZSM5 is used. This limitation can be tackled by the use metal oxide

in a separate bed. Metal oxides are efficient for deoxygenation reaction and tar cracking. With the use of CaO and HZSM-5, an improved yield of aromatic and aliphatic hydrocarbon was observed when LLDPE was co-pyrolyzed with xylan. Ding et al. [73] studied the co-pyrolysis of corn stover and LDPE over CeO_2 and HZSM-5 dual catalyst. The catalytic pyrolysis of corn stover was performed over the CeO_2 bed, followed by conversion to hydrocarbons on the HZSM-5 catalyst. As a result, the H/C ratio was increased by hydrogen supplement from LDPE [55]. Ding et al. [74] employed the dual catalyst bed of CaO and HZSM-5 to convert acids in the pyrolytic products of xylan to valuable hydrocarbons. LLDPE (as a hydrogen source) was co-pyrolyzed with xylan over the HZSM-5 bed during the process. The hydrogen-rich fragments derived from LLDPE promoted the Diels- Alder reactions of furans and participated in the hydrocarbon pool reactions of non-furanic compounds. The metal-doped ZSM-5 was utilized for the co-pyrolysis of biomass and plastics. A series of phosphorous (P) and phosphorous-nickel (P/Ni) modified zeolites were tested for pinewood and low-density polyethylene (LDPE) co-pyrolysis [75]. As a result, an increase in olefins and aromatic hydrocarbons yield to 52.8% and 54.1% in the presence of phosphorous and phosphorous-nickel catalysts, respectively, have been measured compared to 42.9% oil yield without these metal loadings. Moreover, the decrease in biochar yield (from 22.6 C% to 18.9 C%) suggesting that the addition of metals helped improve the oil yield by reducing the hydrocarbons cracking. Furthermore, the impregnation of P and P/Ni improved the hydrothermal stability of ZSM-5 and prevented catalyst deactivation during the co-pyrolysis process.

Ding et al. [73] studied the co-pyrolysis of corn stover and LDPE over CeO_2 and HZSM-5 dual catalyst. The catalytic pyrolysis of corn stover was performed over the CeO_2 bed, followed by conversion to hydrocarbons on the HZSM-5 catalyst. As a result, the H/C ratio was increased by hydrogen supplement from LDPE and promoted hydrocarbon formation. Hwang et al. [76] studied the biomass (i.e., yellow poplar) decomposition both in the presence and absence of potassium and reported a decrease in biomass decomposition temperature from 373.9 °C to 359.0 °C on the increase in potassium concentration. When used in fast catalytic pyrolysis (CFP), the char yield remained doubled regardless of temperature compared to demineralized biomass.

Nevertheless, the dual catalyst layout showed a new opportunity for the efficient conversion of biomass materials into hydrocarbons in the presence of plastic [77]. Xue et al. [78] conducted a segmented co-pyrolysis of biomass and HDPE with $MgCl_2$ and HZSM-5 catalyst in a fixed bed reactor. $MgCl_2$ significantly enhanced the synergistic effect between biomass and HDPE. The maximum bio-oil yield of 43 wt% and aromatics proportion of 95.9 wt% were obtained at 600 °C with biomass to HDPE ratio 1:2 and feedstock to catalyst ratio 1:1 [79]. Further, the bimetallic amorphous catalyst CoNiB remained more active in producing hydrocarbon compounds than individual NiB and CoB [80]. It remained promising for post upgradation of pyrolysis oil (i.e., hydrogenation and hydrodeoxygenation of pyrolysis oil).

Thus, the synergistic effect of biomass and plastic during catalytic co-pyrolysis showed the improved composition of bio-oil, similar to drop-in fuel. It is noteworthy that the biomass materials, when interacted with plastic or its derived compounds over a catalyst surface, resulted in a complex reaction mechanism, which was challenging to analyze. In this context, biomass model compounds such as cellulose, hemicellulose, and lignin were often utilized in catalytic co-pyrolysis studies. Further, the plastic with higher hydrogen carbon ratios (H/C) and a vast resource of hydrogen showed improvement in the yield of bio-oil and hydrocarbon selectivity and the minimization of catalyst deactivation during the co-pyrolysis process; hence it remained attractive [84,85]. The positive synergistic effect of biomass and plastic in catalytic co-pyrolysis improved the yield and composition of bio-oil. The information provided would be crucial to understand the co-pyrolysis of biomass and COVID-19 wastes as it is essentially biomass/plastic materials. As demonstrated recently that the COVID-19 mask can produce hydrocarbon fuels upon pyroylsis [86], which indicates the promising potential of COVID-19 mask in providing the in-situ hydrogen to the biomass-derived compounds during co-pyrolysis, and eventually producing hydrocarbon-rich bio-oil. Similarly, the COVID-19 medical waste comprising of PE, PP, PS, and PET likely to show the synergistic with biomass (with and without catalyst) in a similar way as discussed in this section [87].

5. Economic analysis of biomass and plastic co-pyrolysis: evaluation and recommendation

The fruitful implementation of co-pyrolysis of biomass and plastics/COVID-19 wastes, with and without catalyst, relies on the economics of the overall production process. One of the viable approaches to boost process economics is to perform co-pyrolysis of biomass and plastic/COVID-19 wastes in a distributed way. The decentralized operation of pyrolysis remains inexpensive compared to a centralized plant. It may save a significant percentage of overall cost since biomass feedstock transportation alone takes around 30% of the overall cost. Another approach would be adopting cheaper but product selective catalysts for bio-oil upgradation for co-pyrolysis of biomass/plastics/COVID-19 wastes. Although numerous studies highlighted the cost of bio-oil production during fast pyrolysis, the bio-oil upgradation to transportation fuel is rarely discussed [88–91]. Further, hydrogen during bio-oil upgradation adds additional cost to the overall process; in this context, co-pyrolysis of biomass and plastics/COVID-19 wastes under suitable catalyst eliminates the hydrogen because of its hydrogen-rich nature and thus, minimizes the overall production cost. Further, the understanding of synergistic between biomass and plastic during co-pyrolysis, with and without catalyst, can be anticipated for biomass and COVID-19 waste pyrolysis systems too. It would help the researchers and policymakers tune the operating conditions of the biomass/plastic/COVID-19 co-pyrolysis, producing yield and composition of bio-oil as per the need. This would minimize the trial and error in experimentation and eventually save the operating cost.

To the best of our knowledge, the techno-economic analysis of biomass and plastic co-pyrolysis is rarely available [92]; however, there are multiple reports on the techno-economics biomass fast pyrolysis alone. The initial investment varies significantly with the biomass pyrolysis system and remains difficult to estimate, although different investment approaches have been found in the literature [93–95]. The investment in the pyrolysis process includes biomass pre-treatment and feeder system, pyrolyzer capital and operating cost, product recovery, and storage cost. The studies suggested that the cost of bio-oil obtained from biomass fast pyrolysis ranged between 0.11 and 0.65 US dollar per liter [88,89,91,96,97], which is likely to get reduced in the case of distributed operation of biomass and plastic/COVID-19 waste co-pyrolysis, since it produces better quality bio-oil with less operating cost. Based on the 450 tonnes per day capacity wood fast pyrolysis plant, the capital and operating cost estimated as 48.2 million US dollars and 9.6 million US dollars, respectively, for 106 million liters of bio-oil per year [97]. The co-pyrolysis may cut the operating cost up to some extent by avoiding the biomass and plastic/COVID-19 waste segregation; hence may give better economics than pyrolysis alone.

Further, the co-pyrolysis of biomass and plastic under the catalytic environment mainly utilized the higher amount of catalyst (or low feed to catalyst ratio, feed: catalyst = 1:2–1:20), which remained a hurdle for the large-scale operation [98]. Thus, a higher feed to catalyst ratio is desirable to safeguard the economic viability of the CFP process. Moreover, the catalyst deactivation (via coke formation) during the co-pyrolysis process is commonly observed, which may be avoided to a greater extent using a newly designed noble metal catalyst. Besides, the catalyst regeneration process must be evaluated for improved economics. Concerning the challenges mentioned above, the catalytic co-pyrolysis process is barely reported at the pilot-scale, despite the significant achievement in the micro-scale or lab-scale reactors [99,100]. It is essential to examine the impact of biomass nature, catalyst

type, and operating parameters on CFP of biomass and plastics in real large-scale reactors [98].

Nevertheless, the co-pyrolysis of biomass and plastic (with and without catalyst) appeared as a promising route that aids in waste elimination; more importantly, it avoids the cost of biomass and plastic waste handling and processing. Further, the co-pyrolysis-derived biochar is reportedly used for soil remediation [101], water treatment (or removal of metals from water) [102,103]. The hydrocarbon-rich bio-oil produced from CFP of biomass and plastic would blend with conventional fuel and minimize the burden of the fuel demand to some extent. The gases, especially CO_2 emission, would be less from the burning of bio-oil blended fuel compared to fossil fuel alone. Thus, it will reduce environmental damage and would be beneficial for humankind.

6. Future outlook and perspective

It is evident that co-pyrolysis can be a potential solution to tackle both rural and urban solid waste without further segregation. Indeed, decentralized small co-pyrolysis units can be a game changer for effective solid waste management, especially plastic waste, biomass, and agro residues. However, the composition of plastic and biomass wastes varies drastically; thus, there is an urgent need to study the interaction of oxygenated and non-oxygenated molecules. In this regard, further theoretical studies, including density functional theory for a mechanistic understanding of the overall process, could be interesting for future studies. In addition, economic analysis of such processes, especially for ratios of plastic and biomass, may be an exciting area of research for the commercialization of such technologies. Also, there is a need to study the correlation between liquid oil quality and the composition of combustible gases to develop further insight into the process. Additionally, the discussion on existing biomass and plastic waste issues needs to be understood further for integration [6–8].

It is also worth mentioning that COVID-19 have caused a drastic surge in the generation of solid waste consisting such as face masks, PPE kits, sanitizer bottles, hand gloves, and other personal hygiene-related items in addition to existing biomass and plastic wastes [18]. Most of these items have a very short-term application and are made of plastic/paper/fabric materials [104]. The disposal and treatment of COVID-19 waste created new challenges for humankind and the research fraternity. It is cautioned that infectious COVID-19 waste cannot be recycled under any conditions as per guidelines issued by WHO. However, there exists non-infectious waste such as masks, gloves, face shields, etc. used day to day by uninfected common people that can be recycled after using a suitable disinfectant. Indeed, infectious waste generated due to COVID-19 is insignificant than non-infectious waste generated during this pandemic. Apparently, due to appropriate covid behavior, the face masks, gloves, and sanitizer bottles are being routinely used by people across the globe, leading to massive waste generation. For example, about 80% acceptance rate for facemasks is observed in most African countries [18]. The number of facemasks sold per day is 50% of the world's total population [105]. It is further expected that more than a hundred and a quarter billion facemasks and sixty-five billion gloves will be required every month for the earth's humankind population to deal with the current COVID-19 pandemic [106]. Non-infectious waste generated from non-infected population is mostly free from the coronavirus and, thus, can be tackled with currently available waste disposal technologies such as incineration, combustion, albeit after disinfection using chlorine or any other disinfectant. However, a little discussion is available on the handling and conversion biomass, plastic, and COVID-19 wastes altogether [107]. Therefore, the application of co-pyrolysis can be explored for potential disposal of non-infectious waste arising due to COVID-19, which contains mostly plastic and fibers derived from biomass. However, utmost care should be taken, and non-infectious waste should not be processed without using a suitable disinfectant on it.

7. Conclusions

This review critically discussed the synergistic effect of biomass and plastic during co-pyrolysis. The synergistic effect showed a positive impact on the bio-oil yield and composition. Notably, the hydrocarbon-rich bio-oil was obtained from the co-pyrolysis of biomass and plastic wastes. The percentage of hydrocarbon compounds within bio-oil, either an aliphatic or aromatics, differed significantly for different biomass/plastic systems, their operating conditions, and catalyst. Several reactions (such as depolymerization, dehydration, hydrogenation, hydrodeoxygenation, decarbonylation, decarboxylation, Diels–Alder, reactions, oligomerization, isomerization, aromatization, cyclization, dimerization, -OH radicals elimination, conjugation of C═C bonds, radical coupling reactions, etc.) responsible for bio-oil quality improvement during co-pyrolysis are revealed with and without catalyst. The impact of co-pyrolysis reactor parameters on reactivity and synergistic effect of biomass and plastic derived compounds, and hence bio-oil quality, is discussed. The knowledge on the inter-relation of biomass and plastics concerning hydrocarbon generation may be useful in understanding the co-pyrolysis behavior of non-infectious solid waste arising from COVID-19. The crucial information of interactions between biomass and plastic-derived compounds on zeolite alone, modified zeolite, zeolite with other catalysts, and bimetallic catalysts discussed in this review would instigate multiple researches for biomass and COVID-19 waste co-pyrolysis. The treatment of COVID-19 non-infectious waste through co-pyrolysis may contribute to the safe disposal and minimization.

CRediT authorship contribution statement

Khursheed B. Ansari: Conceptualization, Drafting biomass/plastic synergistic, Economic analysis, Compilation of review. **Ejaz Ahmad**: Introduction and foundation of review, Editing, and proofreading. **Rohidas Bhoi**: Impact of catalysts on biomass/plastic co-pyrolysis, Editing and proofreading. **Saeikh Zaffar Hassan**: Drafting co-pyrolysis reactors process parameters; Editing and proofreading. Permissions for Fig. S1 and Fig. 1[A–C] are obtained.

Declaration of Competing Interest

The authors declare no competing financial interests or personal relationship that could have appeared or influence the work reported in this paper.

Appendix A. Supporting information

Supplementary data associated with this article can be found in the online version at doi:10.1016/j.jece.2021.106436.

References

[1] R. Thomson, P. Kwong, E. Ahmad, K.D.P. Nigam, Clean syngas from small commercial biomass gasifiers; a review of gasifier development, recent advances and performance evaluation, Int. J. Hydrog. Energy 45 (2020) 21087–21111.
[2] S. Quereshi, P.R. Jadhao, A. Pandey, E. Ahmad, K.K. Pant, 1 – Overview of sustainable fuel and energy technologies, in: S. Dutta, C. Mustansar Hussain (Eds.), Sustainable Fuel Technologies Handbook, Academic Press, 2021, pp. 3–25.
[3] K.B. Ansari, V.G. Gaikar, Investigating production of hydrocarbon rich bio-oil from grassy biomass using vacuum pyrolysis coupled with online deoxygenation of volatile products over metallic iron, Renew. Energy 130 (2019) 305–318.
[4] P.R. Jadhao, E. Ahmad, K.K. Pant, K.D.P. Nigam, Environmentally friendly approach for the recovery of metallic fraction from waste printed circuit boards using pyrolysis and ultrasonication, Waste Manag. 118 (2020) 150–160.
[5] N. Singh, Y. Tang, Z. Zhang, C. Zheng, COVID-19 waste management: effective and successful measures in Wuhan, China, Resour. Conserv. Recycl. 163 (2020), 105071.
[6] N. Tripathi, C.D. Hills, R.S. Singh, C.J. Atkinson, Biomass waste utilisation in low-carbon products: harnessing a major potential resource, npj Clim. Atmos. Sci. 2 (2019) 35.

[7] N.M. Clauser, G. González, C.M. Mendieta, J. Kruyeniski, M.C. Area, M. E. Vallejos, Biomass waste as sustainable raw material for energy and fuels, Sustainability 13 (2021) 794.
[8] L. Lebreton, A. Andrady, Future scenarios of global plastic waste generation and disposal, Palgrave Commun. (2019) 6.
[9] S. Quereshi, E. Ahmad, K.K.K. Pant, S. Dutta, Insights into microwave-assisted synthesis of 5-ethoxymethylfurfural and ethyl levulinate using tungsten disulfide as a catalyst, ACS Sustain. Chem. Eng. 8 (2020) 1721–1729.
[10] K.B. Ansari, J.S. Arora, J.W. Chew, P.J. Dauenhauer, S.H. Mushrif, Fast pyrolysis of cellulose, hemicellulose, and lignin: effect of operating temperature on bio-oil yield and composition and insights into the intrinsic pyrolysis chemistry, Ind. Eng. Chem. Res. 58 (2019) 15838–15852.
[11] W.D. Chanaka Udayanga, A. Veksha, A. Giannis, G. Lisak, T.-T. Lim, Effects of sewage sludge organic and inorganic constituents on the properties of pyrolysis products, Energy Convers. Manag. 196 (2019) 1410–1419.
[12] W.D. Chanaka Udayanga, A. Veksha, A. Giannis, T.-T. Lim, Pyrolysis derived char from municipal and industrial sludge: impact of organic decomposition and inorganic accumulation on the fuel characteristics of char, Waste Manag. 83 (2019) 131–141.
[13] E. Ahmad, N. Jäger, A. Apfelbacher, R. Daschner, A. Hornung, K.K. Pant, Integrated thermo-catalytic reforming of residual sugarcane bagasse in a laboratory scale reactor, Fuel Process. Technol. 171 (2018) 277–286.
[14] C. Dorado, C.A. Mullen, A.A. Boateng, Origin of carbon in aromatic and olefin products derived from HZSM-5 catalyzed co-pyrolysis of cellulose and plastics via isotopic labeling, Appl. Catal. B Environ. 162 (2015) 338–345.
[15] N. Sophonrat, L. Sandström, A.-C. Johansson, W. Yang, Co-pyrolysis of mixed plastics and cellulose: an interaction study by Py-GC×GC/MS, Energy Fuels 31 (2017) 11078–11090.
[16] N. Sophonrat, W. Yang, Effect of mixing methods of polyethylene and cellulose on volatile products from its co-pyrolysis, Energy Procedia 142 (2017) 315–320.
[17] H. Hassan, J.K. Lim, B.H. Hameed, Recent progress on biomass co-pyrolysis conversion into high-quality bio-oil, Bioresour. Technol. 221 (2016) 645–655.
[18] C. Nzediegwu, S.X. Chang, Improper solid waste management increases potential for COVID-19 spread in developing countries, Resour. Conserv. Recycl. 161 (2020), 104947.
[19] M.I. Jahirul, M.G. Rasul, A.A. Chowdhury, N. Ashwath, Biofuels production through biomass pyrolysis-a technological review, Energies 5 (2012) 4952–5001.
[20] J.A. Garcia-Nunez, M.R. Pelaez-Samaniego, M.E. Garcia-Perez, I. Fonts, J. Abrego, R.J.M. Westerhof, et al., Historical developments of pyrolysis reactors: a review, Energy Fuels 31 (2017) 5751–5775.
[21] M.R. Barr, R. Volpe, R. Kandiyoti, Influence of reactor design on product distributions from biomass pyrolysis, ACS Sustain. Chem. Eng. 7 (2019) 13734–13745.
[22] M.H.M. Ahmed, N. Batalha, H.M.D. Mahmudul, G. Perkins, M. Konarova, A review on advanced catalytic co-pyrolysis of biomass and hydrogen-rich feedstock: insights into synergistic effect, catalyst development and reaction mechanism, Bioresour. Technol. 310 (2020), 123457.
[23] L. Zhang, Z. Bao, S. Xia, Q. Lu, K.B. Walters, Catalytic pyrolysis of biomass and polymer wastes, Catalysts 8 (2018) 659.
[24] R. Volpe, J.M.B. Menendez, T.R. Reina, A. Messineo, M. Millan, Evolution of chars during slow pyrolysis of citrus waste, Fuel Process. Technol. 158 (2017) 255–263.
[25] B. Han, Y. Chen, Y. Wu, D. Hua, Z. Chen, W. Feng, et al., Co-pyrolysis behaviors and kinetics of plastics–biomass blends through thermogravimetric analysis, J. Therm. Anal. Calorim. 115 (2014) 227–235.
[26] X. Lin, H. Lei, E. Huo, M. Qian, W. Mateo, Q. Zhang, et al., Enhancing jet fuel range hydrocarbons production from catalytic co-pyrolysis of Douglas fir and low-density polyethylene over bifunctional activated carbon catalysts, Energy Convers. Manag. 211 (2020), 112757.
[27] L. Zhou, Y. Wang, Q. Huang, J. Cai, Thermogravimetric characteristics and kinetic of plastic and biomass blends co-pyrolysis, Fuel Process. Technol. 87 (2006) 963–969.
[28] M. Razzaq, M. Zeeshan, S. Qaisar, H. Iftikhar, B. Muneer, Investigating use of metal-modified HZSM-5 catalyst to upgrade liquid yield in co-pyrolysis of wheat straw and polystyrene, Fuel 257 (2019), 116119.
[29] R.K. Mishra, A. Sahoo, K. Mohanty, Pyrolysis kinetics and synergistic effect in co-pyrolysis of Samanea saman seeds and polyethylene terephthalate using thermogravimetric analyser, Bioresour. Technol. 289 (2019), 121608.
[30] S. Maiti, S. Purakayastha, B. Ghosh, Thermal characterization of mustard straw and stalk in nitrogen at different heating rates, Fuel 86 (2007) 1513–1518.
[31] S.-S. Kim, H.V. Ly, J. Kim, J.H. Choi, H.C. Woo, Thermogravimetric characteristics and pyrolysis kinetics of Alga Sagarssum sp. biomass, Bioresour. Technol. 139 (2013) 242–248.
[32] H. Jüntgen, Review of the kinetics of pyrolysis and hydropyrolysis in relation to the chemical constitution of coal, Fuel 63 (1984) 731–737.
[33] X. Zhang, H. Lei, L. Zhu, X. Zhu, M. Qian, G. Yadavalli, et al., Thermal behavior and kinetic study for catalytic co-pyrolysis of biomass with plastics, Bioresour. Technol. 220 (2016) 233–238.
[34] Z. Xiang, J. Liang, H.M. Morgan, Y. Liu, H. Mao, Q. Bu, Thermal behavior and kinetic study for co-pyrolysis of lignocellulosic biomass with polyethylene over cobalt modified ZSM-5 catalyst by thermogravimetric analysis, Bioresour. Technol. 247 (2018) 804–811.
[35] Z. Sebestyén, E. Barta-Rajnai, J. Bozi, M. Blazsó, E. Jakab, N. Miskolczi, et al., Thermo-catalytic pyrolysis of biomass and plastic mixtures using HZSM-5, Appl. Energy 207 (2017) 114–122.
[36] Y. Zheng, J. Wang, C. Liu, Y. Lu, X. Lin, W. Li, et al., Catalytic copyrolysis of metal impregnated biomass and plastic with Ni-based HZSM-5 catalyst: synergistic effects, kinetics and product distribution, Int. J. Energy Res. 44 (2020) 5917–5935.
[37] P. Ghetti, L. Ricca, L. Angelini, Thermal analysis of biomass and corresponding pyrolysis products, Fuel 75 (1996) 565–573.
[38] M. Alam, A. Bhavanam, A. Jana, J.K.S. Viroja, N.R. Peela, Co-pyrolysis of bamboo sawdust and plastic: synergistic effects and kinetics, Renew. Energy 149 (2020) 1133–1145.
[39] X. Kai, R. Li, T. Yang, S. Shen, Q. Ji, T. Zhang, Study on the co-pyrolysis of rice straw and high density polyethylene blends using TG-FTIR-MS, Energy Convers. Manag. 146 (2017) 20–33.
[40] X. Kai, T. Yang, S. Shen, R. Li, TG-FTIR-MS study of synergistic effects during co-pyrolysis of corn stalk and high-density polyethylene (HDPE), Energy Convers. Manag. 181 (2019) 202–213.
[41] P. Lu, Q. Huang, A.C. Bourtsalas, Y. Chi, J. Yan, Synergistic effects on char and oil produced by the co-pyrolysis of pine wood, polyethylene and polyvinyl chloride, Fuel 230 (2018) 359–367.
[42] S. Kumagai, K. Fujita, T. Kameda, T. Yoshioka, Interactions of beech wood–polyethylene mixtures during co-pyrolysis, J. Anal. Appl. Pyrolysis 122 (2016) 531–540.
[43] R.K. Mishra, J.S. Iyer, K. Mohanty, Conversion of waste biomass and waste nitrile gloves into renewable fuel, Waste Manag. 89 (2019) 397–407.
[44] J. Alvarez, M. Amutio, G. Lopez, L. Santamaria, J. Bilbao, M. Olazar, Improving bio-oil properties through the fast co-pyrolysis of lignocellulosic biomass and waste tyres, Waste Manag. 85 (2019) 385–395.
[45] V.I. Sharypov, N. Marin, N.G. Beregovtsova, S.V. Baryshnikov, B.N. Kuznetsov, V. L. Cebolla, et al., Co-pyrolysis of wood biomass and synthetic polymer mixtures. Part I: influence of experimental conditions on the evolution of solids, liquids and gases, J. Anal. Appl. Pyrolysis 64 (2002) 15–28.
[46] M.S. Mettler, D.G. Vlachos, P.J. Dauenhauer, Top ten fundamental challenges of biomass pyrolysis for biofuels, Energy Environ. Sci. 5 (2012) 7797–7809.
[47] D. Hua, Y. Wu, Y. Chen, J. Li, M. Yang, X. Lu, Co-pyrolysis behaviors of the cotton straw/PP mixtures and catalysis hydrodeoxygenation of co-pyrolysis products over Ni-Mo/Al2O3 catalyst, Catalysts 5 (2015) 2085–2097.
[48] Y. Xue, S. Zhou, R.C. Brown, A. Kelkar, X. Bai, Fast pyrolysis of biomass and waste plastic in a fluidized bed reactor, Fuel 156 (2015) 40–46.
[49] E. Önal, B.B. Uzun, A.E. Pütün, Bio-oil production via co-pyrolysis of almond shell as biomass and high density polyethylene, Energy Convers. Manag. 78 (2014) 704–710.
[50] X. Li, H. Zhang, J. Li, L. Su, J. Zuo, S. Komarneni, et al., Improving the aromatic production in catalytic fast pyrolysis of cellulose by co-feeding low-density polyethylene, Appl. Catal. A Gen. 455 (2013) 114–121.
[51] D.K. Ojha, R. Vinu, Fast co-pyrolysis of cellulose and polypropylene using Py-GC/MS and Py-FT-IR, RSC Adv. 5 (2015) 66861–66870.
[52] P. Rutkowski, A. Kubacki, Influence of polystyrene addition to cellulose on chemical structure and properties of bio-oil obtained during pyrolysis, Energy Convers. Manag. 47 (2006) 716–731.
[53] M. Brebu, S. Ucar, C. Vasile, J. Yanik, Co-pyrolysis of pine cone with synthetic polymers, Fuel 89 (2010) 1911–1918.
[54] E. Jakab, M. Blazsó, O. Faix, Thermal decomposition of mixtures of vinyl polymers and lignocellulosic materials, J. Anal. Appl. Pyrolysis 58–59 (2001) 49–62.
[55] S. Kumagai, K. Fujita, Y. Takahashi, T. Kameda, Y. Saito, T. Yoshioka, Impacts of pyrolytic interactions during the co-pyrolysis of biomass/plastic: synergies in lignocellulose-polyethylene system, J. Jpn. Inst. Energy 98 (2019) 202–219.
[56] M. Asmadi, H. Kawamoto, S. Saka, Gas- and solid/liquid-phase reactions during pyrolysis of softwood and hardwood lignins, J. Anal. Appl. Pyrolysis 92 (2011) 417–425.
[57] D.K. Shen, S. Gu, K.H. Luo, S.R. Wang, M.X. Fang, The pyrolytic degradation of wood-derived lignin from pulping process, Bioresour. Technol. 101 (2010) 6136–6146.
[58] J. Yang, J. Rizkiana, W.B. Widayatno, S. Karnjanakom, M. Kaewpanha, X. Hao, et al., Fast co-pyrolysis of low density polyethylene and biomass residue for oil production, Energy Convers. Manag. 120 (2016) 422–429.
[59] D. Supramono, M.A. Nabil, Setiadi, M. Nasikin, Effect of feed composition of co-pyrolysis of corncobs–polypropylene plastic on mass interaction between biomass particles and plastics, IOP Conf. Ser. Earth Environ. Sci. 105 (2018), 012049.
[60] P. Ghorbannezhad, S. Park, J.A. Onwudili, Co-pyrolysis of biomass and plastic waste over zeolite- and sodium-based catalysts for enhanced yields of hydrocarbon products, Waste Manag. 102 (2020) 909–918.
[61] Z. Wang, K.G. Burra, T. Lei, A.K. Gupta, Co-pyrolysis of waste plastic and solid biomass for synergistic production of biofuels and chemicals-a review, Prog. Energy Combust. Sci. 84 (2021), 100899.
[62] T.C. Hoff, D.W. Gardner, R. Thilakaratne, J. Proano-Aviles, R.C. Brown, J.-P. Tessonnier, Elucidating the effect of desilication on aluminum-rich ZSM-5 zeolite and its consequences on biomass catalytic fast pyrolysis, Appl. Catal. A Gen. 529 (2017) 68–78.
[63] Y.-T. Cheng, G.W. Huber, Production of targeted aromatics by using Diels–Alder classes of reactions with furans and olefins over ZSM-5, Green Chem. 14 (2012) 3114–3125.
[64] N. Nikbin, P.T. Do, S. Caratzoulas, R.F. Lobo, P.J. Dauenhauer, D.G. Vlachos, A DFT study of the acid-catalyzed conversion of 2,5-dimethylfuran and ethylene to p-xylene, J. Catal. 297 (2013) 35–43.
[65] L.E. Overman, R.L. Freerks, C.B. Petty, L.A. Clizbe, R.K. Ono, G.F. Taylor, et al., Diels-Alder reactions of 1-(acylamino)-1,3-dienes, J. Am. Chem. Soc. 103 (1981) 2816–2822.

[66] D. Duan, Y. Wang, L. Dai, R. Ruan, Y. Zhao, L. Fan, et al., Ex-situ catalytic co-pyrolysis of lignin and polypropylene to upgrade bio-oil quality by microwave heating, Bioresour. Technol. 241 (2017) 207–213.
[67] T.R. Carlson, T.P. Vispute, G.W. Huber, Green gasoline by catalytic fast pyrolysis of solid biomass derived compounds, ChemSusChem 1 (2008) 397–400.
[68] X. Bai, P. Johnston, S. Sadula, R.C. Brown, Role of levoglucosan physiochemistry in cellulose pyrolysis, J. Anal. Appl. Pyrolysis 99 (2013) 58–65.
[69] C.L. Williams, C.-C. Chang, P. Do, N. Nikbin, S. Caratzoulas, D.G. Vlachos, et al., Cycloaddition of biomass-derived furans for catalytic production of renewable p-xylene, ACS Catal. 2 (2012) 935–939.
[70] Y.-K. Park, B. Lee, A. Watanabe, H.W. Lee, J.Y. Lee, S. Kim, et al., Catalytic copyrolysis of cork oak and waste plastic films over Hbeta, Catalysts 8 (2018) 318.
[71] Y.-M. Kim, J. Jae, B.-S. Kim, Y. Hong, S.-C. Jung, Y.-K. Park, Catalytic co-pyrolysis of torrefied yellow poplar and high-density polyethylene using microporous HZSM-5 and mesoporous Al-MCM-41 catalysts, Energy Convers. Manag. 149 (2017) 966–973.
[72] H. Zhang, R. Xiao, J. Nie, B. Jin, S. Shao, G. Xiao, Catalytic pyrolysis of black-liquor lignin by co-feeding with different plastics in a fluidized bed reactor, Bioresour. Technol. 192 (2015) 68–74.
[73] K. Ding, A. He, D. Zhong, L. Fan, S. Liu, Y. Wang, et al., Improving hydrocarbon yield via catalytic fast co-pyrolysis of biomass and plastic over ceria and HZSM-5: an analytical pyrolyzer analysis, Bioresour. Technol. 268 (2018) 1–8.
[74] K. Ding, Z. Zhong, J. Wang, B. Zhang, L. Fan, S. Liu, et al., Improving hydrocarbon yield from catalytic fast co-pyrolysis of hemicellulose and plastic in the dual-catalyst bed of CaO and HZSM-5, Bioresour. Technol. 261 (2018) 86–92.
[75] W. Yao, J. Li, Y. Feng, W. Wang, X. Zhang, Q. Chen, et al., Thermally stable phosphorus and nickel modified ZSM-5 zeolites for catalytic co-pyrolysis of biomass and plastics, RSC Adv. 5 (2015) 30485–30494.
[76] H. Hwang, S. Oh, T.-S. Cho, I.-G. Choi, J.W. Choi, Fast pyrolysis of potassium impregnated poplar wood and characterization of its influence on the formation as well as properties of pyrolytic products, Bioresour. Technol. 150 (2013) 359–366.
[77] H. Zhang, P.K.W. Likun, R. Xiao, Improving the hydrocarbon production via co-pyrolysis of bagasse with bio-plastic and dual-catalysts layout, Sci. Total Environ. 618 (2018) 151–156.
[78] X. Xue, Z. Pan, C. Zhang, D. Wang, Y. Xie, R. Zhang, Segmented catalytic co-pyrolysis of biomass and high-density polyethylene for aromatics production with MgCl2 and HZSM-5, J. Anal. Appl. Pyrolysis 134 (2018) 209–217.
[79] S. Zhong, B. Zhang, C. Liu, A. Shujaa aldeen, Mechanism of synergistic effects and kinetics analysis in catalytic co-pyrolysis of water hyacinth and HDPE, Energy Convers. Manag. 228 (2021), 113717.
[80] B.-J. Liaw, C.-H. Chen, Y.-Z. Chen, Hydrogenation of fructose over amorphous nano-catalysts of CoNiB and polymer-stabilized CoNiB, Chem. Eng. J. 157 (2010) 140–145.
[81] K. Praveen Kumar, S. Srinivas, Catalytic co-pyrolysis of biomass and plastics (polypropylene and polystyrene) using spent FCC catalyst, Energy Fuels 34 (2020) 460–473.
[82] X. Lin, Z. Zhang, Z. Zhang, J. Sun, Q. Wang, C.U. Pittman, Catalytic fast pyrolysis of a wood-plastic composite with metal oxides as catalysts, Waste Manag. 79 (2018) 38–47 (New York, NY).
[83] K. Ding, A. He, D. Zhong, L. Fan, S. Liu, Y. Wang, et al., Improving hydrocarbon yield via catalytic fast co-pyrolysis of biomass and plastic over ceria and HZSM-5: an analytical pyrolyzer analysis, Bioresour. Technol. 268 (2018) 1–8.
[84] H. Zhang, J. Zheng, R. Xiao, D. Shen, B. Jin, G. Xiao, et al., Co-catalytic pyrolysis of biomass and waste triglyceride seed oil in a novel fluidized bed reactor to produce olefins and aromatics integrated with self-heating and catalyst regeneration processes, RSC Adv. 3 (2013) 5769–5774.
[85] C. Dorado, C.A. Mullen, A.A. Boateng, H-ZSM5 catalyzed co-pyrolysis of biomass and plastics, ACS Sustain. Chem. Eng. 2 (2014) 301–311.
[86] C. Park, H. Choi, K.-Y. Andrew Lin, E.E. Kwon, J. Lee, COVID-19 mask waste to energy via thermochemical pathway: effect of co-feeding food waste, Energy 230 (2021), 120876.
[87] S. Dharmaraj, V. Ashokkumar, R. Pandiyan, H.S. Halimatul Munawaroh, K. W. Chew, W.-H. Chen, et al., Pyrolysis: an effective technique for degradation of COVID-19 medical wastes, Chemosphere 275 (2021), 130092.
[88] M.N. Islam, F.N. Ani, Techno-economics of rice husk pyrolysis, conversion with catalytic treatment to produce liquid fuel, Bioresour. Technol. 73 (2000) 67–75.
[89] M.L. Cottam, A.V. Bridgwater, Techno-economic modelling of biomass flash pyrolysis and upgrading systems, Biomass Bioenergy 7 (1994) 267–273.
[90] Y. Solantausta, D. Beckman, A.V. Bridgwater, J.P. Diebold, D.C. Elliott, Assessment of liquefaction and pyrolysis systems, Biomass Bioenergy 2 (1992) 279–297.
[91] C.E. Gregoire, R.L. Bain, Technoeconomic analysis of the production of biocrude from wood, Biomass Bioenergy 7 (1994) 275–283.
[92] T. Kuppens, T. Cornelissen, R. Carleer, J. Yperman, S. Schreurs, M. Jans, et al., Economic assessment of flash co-pyrolysis of short rotation coppice and biopolymer waste streams, J. Environ. Manag. 91 (2010) 2736–2747.
[93] J.G. Brammer, M. Lauer, A.V. Bridgwater, Opportunities for biomass-derived "bio-oil" in European heat and power markets, Energy Policy 34 (2006) 2871–2880.
[94] A.V. Bridgwater, A.J. Toft, J.G. Brammer, A techno-economic comparison of power production by biomass fast pyrolysis with gasification and combustion, Renew. Sustain. Energy Rev. 6 (2002) 181–246.
[95] R.V. Siemons, A Development Perspective for Biomass-Fuelled Electricity Generation Technologies Economic Technology Assessment in View of Sustainability, 2002.
[96] R.P. Anex, A. Aden, F.K. Kazi, J. Fortman, R.M. Swanson, M.M. Wright, et al., Techno-economic comparison of biomass-to-transportation fuels via pyrolysis, gasification, and biochemical pathways, Fuel 89 (2010) S29–S35.
[97] M.M. Wright, D.E. Daugaard, J.A. Satrio, R.C. Brown, Techno-economic analysis of biomass fast pyrolysis to transportation fuels, Fuel 89 (2010) S2–S10.
[98] H.W. Ryu, D.H. Kim, J. Jae, S.S. Lam, E.D. Park, Y.-K. Park, Recent advances in catalytic co-pyrolysis of biomass and plastic waste for the production of petroleum-like hydrocarbons, Bioresour. Technol. 310 (2020), 123473.
[99] A.-C. Johansson, L. Sandström, O.G.W. Öhrman, H. Jilvero, Co-pyrolysis of woody biomass and plastic waste in both analytical and pilot scale, J. Anal. Appl. Pyrolysis 134 (2018) 102–113.
[100] O. Sanahuja-Parejo, A. Veses, J.M. López, R. Murillo, M.S. Callén, T. García, Ca-based catalysts for the production of high-quality bio-oils from the catalytic co-pyrolysis of grape seeds and waste tyres, Catalysts 9 (2019) 992.
[101] R. Gao, H. Hu, Q. Fu, Z. Li, Z. Xing, U. Ali, et al., Remediation of Pb, Cd, and Cu contaminated soil by co-pyrolysis biochar derived from rape straw and orthophosphate: speciation transformation, risk evaluation and mechanism inquiry, Sci. Total Environ. 730 (2020), 139119.
[102] Y. Li, H. Yu, L. Liu, H. Yu, Application of co-pyrolysis biochar for the adsorption and immobilization of heavy metals in contaminated environmental substrates, J. Hazard. Mater. 420 (2021), 126655.
[103] X. Fan, J. Zhang, Y. Xie, D. Xu, Y. Liu, J. Liu, et al., Biochar produced from the co-pyrolysis of sewage sludge and waste tires for cadmium and tetracycline adsorption from water, Water Sci. Technol. 83 (2021) 1429–1445.
[104] A. Tripathi, V.K. Tyagi, V. Vivekanand, P. Bose, S. Suthar, Challenges, opportunities and progress in solid waste management during COVID-19 pandemic, Case Stud. Chem. Environ. Eng. 2 (2020), 100060.
[105] S. Sangkham, Face mask and medical waste disposal during the novel COVID-19 pandemic in Asia, Case Stud. Chem. Environ. Eng. 2 (2020), 100052.
[106] A.L. Patrício Silva, J.C. Prata, T.R. Walker, A.C. Duarte, W. Ouyang, D. Barcelò, et al., Increased plastic pollution due to COVID-19 pandemic: challenges and recommendations, Chem. Eng. J. 405 (2021), 126683.
[107] S.A. Sarkodie, P.A. Owusu, Impact of COVID-19 pandemic on waste management, Environ. Dev. Sustain. (2020).